



Photolytic and photocatalytic degradation of febantel in aqueous media

Mirta Čizmić^{a,*}, Davor Ljubas^b, Irena Škorić^c, Marko Rožman^{d,e}, Danijela Ašperger^a, Lidija Čurković^f, Mira Petrović^{e,g}, Sandra Babić^a

^aDepartment of Analytical Chemistry, Faculty of Chemical Engineering and Technology, University of Zagreb, Marulićev trg 19, 10000 Zagreb, Croatia, Tel. +385 1 4597 203; Fax: +385 1 4597 250; email: mzrncic@fkit.hr (M. Čizmić)

^bDepartment of Energy, Power Engineering and Environment, Faculty of Mechanical Engineering and Naval Architecture, University of Zagreb, Zagreb, Croatia

^cDepartment of Organic Chemistry, Faculty of Chemical Engineering and Technology, University of Zagreb, Zagreb, Croatia

^dLaboratory for Mass Spectrometry, Division of Physical Chemistry, Ruđer Bošković Institute, Zagreb, Croatia

^eCatalan Institute for Water Research (ICRA), Girona, Spain

^fDepartment of Materials, Faculty of Mechanical Engineering and Naval Architecture, University of Zagreb, Zagreb, Croatia

^gCatalan Institution for research and advanced studies (ICREA), Barcelona, Spain

Received 25 September 2017; Accepted 11 January 2018

ABSTRACT

This research deals with photolytic (UV-C, 254 nm and UV-A, 365 nm) and photocatalytic degradation of anthelmintic drug febantel. In photocatalytic experiments, TiO₂ was used as a catalyst in the form of a nanostructured thin film. UV-C irradiation proved to be effective during photolytic and photocatalytic degradation. The most effective process proved to be photocatalytic degradation with UV-C radiation and febantel half-life time was 2.10 min. During the photocatalytic degradation process nine degradation products were detected. High resolution mass spectrometry data were used to propose degradation products structural formulae and corresponding degradation pathways. The main degradation processes are the hydroxylation of the phenyl ring of febantel and methoxyacetamide substituent reduction in febantel. Toxicity of the samples during photocatalysis was investigated using *Vibrio fischeri* bacteria. Samples showed increase in toxicity as the process advanced which can be attributed to the formation of methyl carbamate derivatives as the degradation products.

Keywords: Anthelmintics; Photocatalysis; Liquid chromatography; High resolution mass spectrometry; *Vibrio fischeri* toxicity

1. Introduction

Pharmaceuticals are molecules with different physico-chemical and biological properties and functionalities. They have an important role in treatment and prevention of disease both in humans and in animals. Pharmaceuticals and their metabolites are being continually introduced in the environment via different pathways [1,2]. The source of their discharge to the environment can be divided into two ways: point source pollution and diffuse pollution. Point source pollution is a single source that can be easily identified and

which originates from separate locations such as industrial effluent, hospital effluent, sewage treatment plants and septic tanks. On the other hand, for diffuse pollution it is hard to identify the exact location. Examples are runoff such as agricultural runoff from the animal waste and manure or urban runoff from domestic waste [3]. The most important source of release of pharmaceuticals into the aquatic environment is by domestic and hospital wastewaters. These waters contain not only the main compound but also metabolites and conjugates formed after consumption and transformations during the metabolite processes in the body [4]. Regardless of the way they are introduced to the environment, most of the pharmaceuticals end up in the aquatic systems. Since surface waters are often used as a source for drinking water

* Corresponding author.

production, the concern on presence of pharmaceuticals in aquatic environment is directly connected to the influence they may have on human health [5]. Vast usage of veterinary pharmaceuticals is either to prevent and to treat disease or as growth promoters results in their indubitable presence in the environment. Because of their nature, they can also have unintended effects on non-target animals and micro-organisms in the environment [6].

Anthelmintic drugs, such as febantel, are the most often used pharmaceuticals in veterinary practice. Febantel (*N*-{[2,3-bis-(methoxycarbonyl)-guanido]-5-(phenylthio)-phenyl}-2-methoxyacetamide) is an anthelmintic agent active against a range of gastrointestinal parasites in animals [7]. According to its chemical structure it belongs to the group of diphenylsulfide anthelmintic drugs. They are administered to a wide range of animals in agriculture and aquaculture for treatment against parasites such as nematodes and arthropods [8,9]. After administration the molecule is partly metabolized in the organism and consequently excreted. The molecule and the newly formed metabolites end up in wastewaters of livestock wastewater treatment plants. The investigated concentrations in influent has been reported as $143 \mu\text{g L}^{-1}$ and the same study reported that most of the investigated anthelmintics showed insignificant or inconsistent removal patterns with large variation [10]. Once in the environment they may have possible negative effects on the living organisms – despite that only a few papers deal with the environmental fate and behavior of the anthelmintic drugs [11–16]. In order to prevent their entry into the environment it is necessary to improve existing wastewater treatment.

Among new technologies for the elimination of emerging contaminants such as pharmaceuticals, advanced oxidation processes (AOPs) are frequently considered to be one of the most promising technologies [17]. Leading AOPs are heterogeneous and homogeneous photocatalysis based on near ultraviolet or solar visible irradiation, ozonation, the Fenton's reagent, ultrasound and wet air oxidation. AOPs rely on hydroxyl radicals (OH^{\bullet}) as highly reactive, non-selective oxidants that readily oxidize many organic compounds [18]. Although destruction of contaminants is generally efficient, the main concern is the formation of transformation products that retain harmful biological activity. Continued oxidation ultimately produces carbon dioxide or other semivolatile carbon products. Recent investigations have increasingly focused on the two AOPs that can be powered by solar radiation, that is, homogeneous catalysis relying on photo-Fenton reactions and heterogeneous catalysis using UV/ TiO_2 process.

Therefore, in this study we present the photolytic and photocatalytic (as a part of AOPs) degradation kinetics of anthelmintic drug febantel in aqueous media. The photodegradation products were identified and monitored along irradiation time using liquid chromatography coupled to high resolution mass spectrometry. In addition, during the photocatalysis real-time toxicity evaluation was performed. To the best of our knowledge, this is the first study assessing degradation kinetics of febantel after AOP, identifying transformation products and evaluating their toxicity. The final results of this research give complete insight of the degradation process of febantel including efficiency, newly formed compounds and toxicity evaluation. Also, TiO_2 was used as photocatalyst in a form of a film instead of slurry which

makes this research more favorable when considering application to existing water treatment processes.

2. Materials and methods

2.1. Materials and reagents

Analytical standard of febantel was obtained from Veterina Animal Health (Kalinovica, Croatia). For chromatographic analysis, methanol (J.T. Baker, Deventer, Netherlands), acetonitrile (J.T. Baker, Deventer, Netherlands) and formic acid (Merck, Darmstadt, Germany) were used. All solvents used were HPLC-grade. Ultrapure water was prepared by a Millipore Simplicity UV system (Millipore Corporation, Billerica, MA, USA) and was used for all experiments. Febantel stock solution concentration of 1 g L^{-1} was prepared by weighing accurate mass of febantel standard and dissolving in acetonitrile. Prepared stock solution was kept in the dark at 4°C . The concentration of aqueous solution of febantel was 1 mg L^{-1} for kinetic studies and the concentration of aqueous solution for investigating degradation products was 10 mg L^{-1} . Both of the solutions were prepared from stock solution and kept in the dark below 4°C until the experiments. The bacterial assay used was the commercially available system LUMISMINI luminescent bacteria test LCK 484 complete with reactivation solution (Hach Lange, Varaždin, Croatia).

2.2. Photolytic and photocatalytic experiments

All experiments were carried out in the 0.11 L borosilicate glass cylinder reactor (with 200 mm in height and 30 mm in diameter). A scheme of the reactor was published elsewhere [19].

The experiments of febantel degradation were carried out at a temperature of $25^{\circ}\text{C} \pm 0.2^{\circ}\text{C}$ using water bath with thermostat control. The experiments were conducted at neutral conditions (no adjustment of pH) with continuous purging with air (O_2), using two different conditions:

- Under UV illumination (photolysis).
- Under UV illumination in the presence of sol-gel TiO_2 film (photocatalysis).

The TiO_2 nanostructured film was deposited on inner reactor surface by sol-gel method and dip-coating technique, described in detail elsewhere [20]. Photocatalytic experiments were conducted using UV-C and UV-A radiation and TiO_2 film. The investigated solution was irradiated with two different wavelengths and the degradation of febantel was monitored: UV-C radiation (254 nm) and UV-A radiation (365 nm).

Two different UV-radiation lamps were used: model Pen-Ray 90-0019-04 with $\lambda_{\text{max}} = 365 \text{ nm}$ and incident photon flux $N_p = 4.295 \times 10^{-6} \text{ Einstein s}^{-1}$ (UV-A lamp) and model Pen-Ray 90-0004-07 with $\lambda_{\text{max}} = 254 \text{ nm}$ (UV-C lamp) and incident photon flux $N_p = 1.033 \times 10^{-6} \text{ Einstein s}^{-1}$ (UVP, Upland, CA, USA). Incident photon flux was determined by actinometric experiments following the procedure described in Kuhn et al. [21]. The lamp was placed in the center of reactor and the UV radiation reaches the inner wall of the reactor through the solution, causing the photolytic/photocatalytic

oxidation process in reactor. During the experiments, samples for chromatographic analysis were taken from the reactor at particular time intervals and stored in dark below 4°C until analysis.

2.3. HPLC/ESI-QqQ-MS analysis

Samples from the photodegradation experiments for kinetics investigations were analyzed on an Agilent Series 1200 HPLC system (Santa Clara, CA, USA) connected to a triple quadrupole mass spectrometer (QqQ) Agilent 6410 with an electrospray ionization (ESI) interface. The column used for chromatographic separation of the degradation products was Synergi Polar C18 (100 mm × 2.0 mm, particle size 2.5 μm) supplied by Phenomenex (Torrance, CA, USA). The mobile phase was MilliQ water acidified with 0.1% formic acid (A) and acetonitrile also acidified with 0.1% formic acid (B). The gradient elution was started with 8% of B which was held for 3 min. During the next 12 min the percentage of B was increased linearly to 95% and was held for 5 min. During 0.01 min it was set to 0% of B and was held for 10 min for equilibration of column. The analyses were performed in the positive ion mode. The conditions of the ion source of the mass spectrometer were: drying gas temperature 350°C, capillary voltage 4 kV, drying gas flow 11 L min⁻¹ and nebulizer pressure 35 psi. Injection volume was 5 μL. For acquisition and data processing Agilent MassHunter software version B.01.03 was used.

Limit of quantification for febantel was 0.17 mg L⁻¹, determined as the concentration where signal to noise ratio was 10.

2.4. HPLC/ESI-LTQ-MS analysis

HPLC-MS and MS/MS experiments for identification of photodegradation products were performed on a LTQ-Orbitrap Velos™ (linear trap quadrupole) coupled with the Aria TLX-1 HPLC system (Thermo Fisher Scientific Inc., USA). Sample mixture was loaded (20 μL injection volume) on Acquity UPLC HSS T₃ (2.1 mm × 50 mm, 1.8 μm particle size, Waters, UK) column where the chromatographic separation was achieved using a 8 min linear gradient from 5% to 95% methanol in 0.1% formic acid at the flow rate of 200 μL min⁻¹. The sample injection, separation and spectra acquisition were carried out automatically. The electrospray capillary voltage was set as 4 kV, capillary temperature was at 300°C, *m/z* range from 100 to 1,000, the instrument resolution was 100,000 at 400 *m/z* and mass accuracy within error of ±5 ppm. Tandem mass spectrometry experiments were performed using collision induced dissociation. Mass range was from 100 to 600 *m/z*, isolation width was 1 Da with normalized collision energy of 35 V and activation time of 30 ms. Nitrogen was used as the collision gas. The acquisition software was set up in auto MS/MS mode using three precursor ions with active exclusion (precursor exclusion after 5 MS/MS spectra for 20 s). Data extraction and analysis were done using Thermo Xcalibur 2.2 SP1.48 (Thermo Fisher Scientific Inc., USA), MZmine2.17 [22] and parts of Bquant script [23].

2.5. Toxicity evaluation with *Vibrio fischeri* bacteria

The acute toxicity evaluation in this study was based on a bioluminescent method of short duration (30 min) according

to DIN 38412-L-34. *Vibrio fischeri* was used as test organisms. The intensity of bacteria luminescence in the analyzed samples was measured on luminometer LUMISTox 300 (Hach Lange, Germany) using the method of geometric progression dilution with 2% NaCl solution used for resuspension. Inhibition (*I*, %) was determined by comparing the intensity of luminescence of a saline control solution with the intensity of luminescence of the diluted sample. Measurements were conducted below 15°C ± 1°C.

3. Results and discussion

3.1. Photolytic and photocatalytic degradation of febantel

Kinetic studies of photolytic and photocatalytic degradation of febantel were made using aqueous solution with concentration of 1 mg L⁻¹. The obtained results are presented in Fig. 1 as the integrated area of the chromatographic peak at the specific time (*A*) divided by the integrated area of the chromatographic peak of febantel at *t* = 0 min (*A*₀). Influence of febantel concentration on degradation rate of photocatalytic process with 254 nm radiation was investigated using higher concentration of febantel (10 mg L⁻¹).

In all experiments the degradation profiles fit a pseudo-first-order kinetic model for the specified time

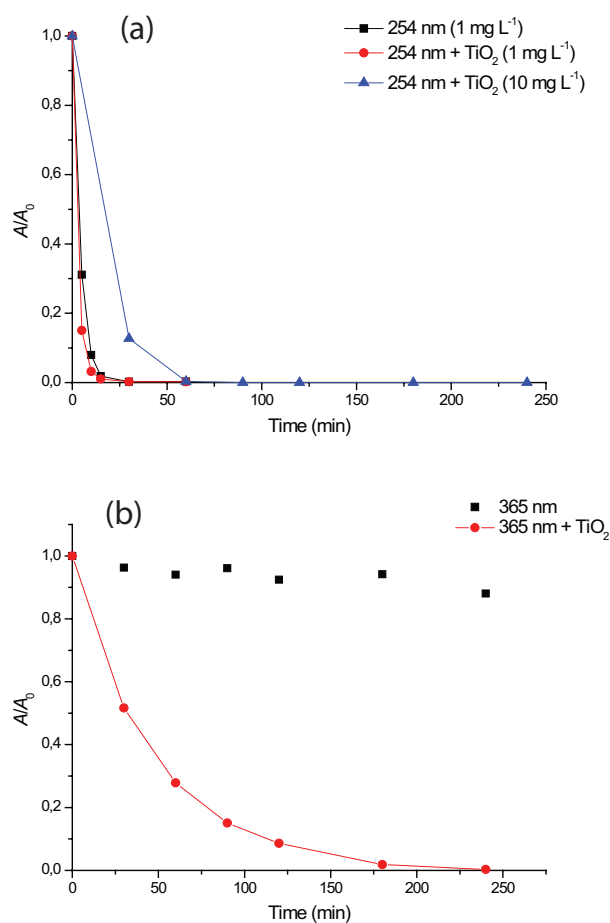


Fig. 1. Photolytic and photocatalytic degradation profiles of febantel below 254 nm (A) and 365 nm (B) irradiation.

intervals. Using \ln – linear plot gathered results were presented and kinetic parameters for degradation of febantel were calculated using linear regression (Table 1). The rate constants, correlation coefficients and half-life times ($t_{1/2} = \ln(2)/k$) are shown for each experiment. In all cases r^2 values were higher than 0.98 indicating that the pseudo-first-order kinetic model describes well the degradation of febantel under investigated experimental conditions.

UV-C radiation treatments resulted with highest febantel degradation rate constants, Fig. 1(A) and Table 1. The influence of the TiO_2 catalyst, when UV-C radiation is used, on the degradation process is observable, but rather low in comparison with the process of direct photolysis. The difference in photolytic and photocatalytic degradation rate can be explained that the remaining photon flux reaches the walls of the reactor and initiates photocatalytic reaction which brings to faster degradation. The increase in the starting concentration of febantel from 1 to 10 mg L^{-1} resulted in increase in degradation rate and it was completely degraded after three times more time (60 min). More photons and more reactive species formed during the photocatalytic reactions are necessary to degrade higher quantity of febantel which results in longer degradation.

The photolytic experiment under UV-A radiation (Fig. 1(B)) showed that degradation of febantel was negligible. Since febantel absorbs no radiation of wavelength above 350 nm (Supplementary material, Fig. S1) therefore it cannot be degraded by direct photolysis using UV-A radiation (365 nm). However, when TiO_2 as a catalyst on the reactor walls is used together with radiation of 365 nm the degradation of febantel occurs. The radiation of wavelength of 365 nm possesses enough energy to activate the photocatalytic oxidation/reduction process on the TiO_2 surface [24,25] which results in the degradation of febantel. While in the case of UV-C radiation without TiO_2 film the photolytic process is dominant, the reaction that occurs in photocatalytic system is the reaction of excitation and the formation of electron–hole pairs on TiO_2 film. This reaction then initiates a sequence of different reactions and one of them is the formation of hydroxyl radicals, OH^\cdot . They are primary oxidants in the photocatalytic oxidation of organic compounds with the UV-A radiation. Direct hole–organic compound reaction is possible but not crucial for degradation of organic compounds [26].

The difference in degradation rates of febantel, when exposed to UV-C or UV-A light, can be partly explained by the absorption spectra of febantel standard solution. Also, the radiation at lower wavelengths has higher radiant energy (Planck's equation [27]).

Table 1
Parameters of the pseudo-first-order kinetic model for the photolysis and photocatalysis of febantel

	k (min^{-1})	r^2	$t_{1/2}$ (min)
UV-C (1 mg L^{-1})	0.248	0.9991	2.79
UV-C + TiO_2 (1 mg L^{-1})	0.330	0.9950	2.10
UV-C + TiO_2 (10 mg L^{-1})	0.102	0.9817	6.80
UV-A + TiO_2 (1 mg L^{-1})	0.023	0.9906	30.14

3.2. Characterization of febantel photodegradation products

Degradation paths of febantel were monitored using HPLC coupled to high resolution mass spectrometry. Degradation products were investigated for photocatalytic degradation with UV-C radiation as it proved to be the most successful process for febantel degradation. These results were compared to results after photocatalytic degradation with UV-A radiation to compare the formed products.

In order to completely define degradation process it was necessary to investigate possible degradation products that evolve during such degradation. Nine degradation products were detected during the investigated degradation processes as newly formed peaks on the chromatogram (Fig. 2).

In order to elucidate the febantel photocatalytic degradation pathways, structures of degradation products (DP) were suggested, primarily on the basis of mass spectra which were very informative. Photocatalytic degradation process with UV-C radiation of anthelmintic drug febantel gives photodegradation products DP1–DP9, as shown in Fig. 3.

Several processes can be suggested primarily from febantel showing the molecular ion m/z 447. These are the hydroxylation of one of the phenyl rings of febantel to DP1 besides methoxyacetamide substituent reduction in febantel. From the hydroxylated diphenylsulfide structure in DP1 secondary degradation product DP3 with lower mass characteristics was obtained. This proposed path includes the cleavage of carbon–sulfur bond in the diphenylsulfide part of the structure giving degradation product DP3, than consequent disappearance of the carbamate side chain giving again DP2 and the final reduced degradation molecule DP4. The obtained results revealed that investigated febantel underwent rapid photodegradation to the related phenol, carboxy, hydroxy and carbamate derivatives.

The structure of the photodegradation product DP1 is supported by the molecular ion m/z 462, for 16 higher than the molecular ion for febantel, obtained as the result of primary hydroxylation process probably of the already substituted phenyl ring in the diphenylsulfide part of the molecule, due to the detection of the further degradation products DP3 and DP6. Product DP3 was suggested according to mass spectrum by molecular ion m/z 355 for 107 lower than m/z for DP1, obtained after the cleavage of carbon–sulfur bond in the diphenylsulfide part of the structure in the second photocatalytic degradation step. In the third photodegradation step, the dehydroxylation of the phenyl ring in DP3 gives the product DP5 showing molecular ion m/z 339 for 16 lower than the m/z for DP3, besides the carbamate side chain separation to give DP2 with m/z 176 and its reduction to the final degradation molecule DP4 with the corresponding mass of molecular ion m/z 118.

Product DP6 with the mass of molecular ion m/z 305 for 157 lower than those of DP1 is explained by the reduction of the carbamate side chain in the primary degradation product DP1 to the amino group as substituent on the hydroxylated diphenylsulfide structure of DP6.

The structure of the degradation product DP7, with the mass characteristics of molecular ion m/z 375, could be explained and obtained through the reduction of the methoxyacetamide substituent in the starting molecule of febantel. The partial reduction of the methoxyacetamide substituent in the starting molecule of febantel can explain the degradation product DP8 showing the mass of molecular ion

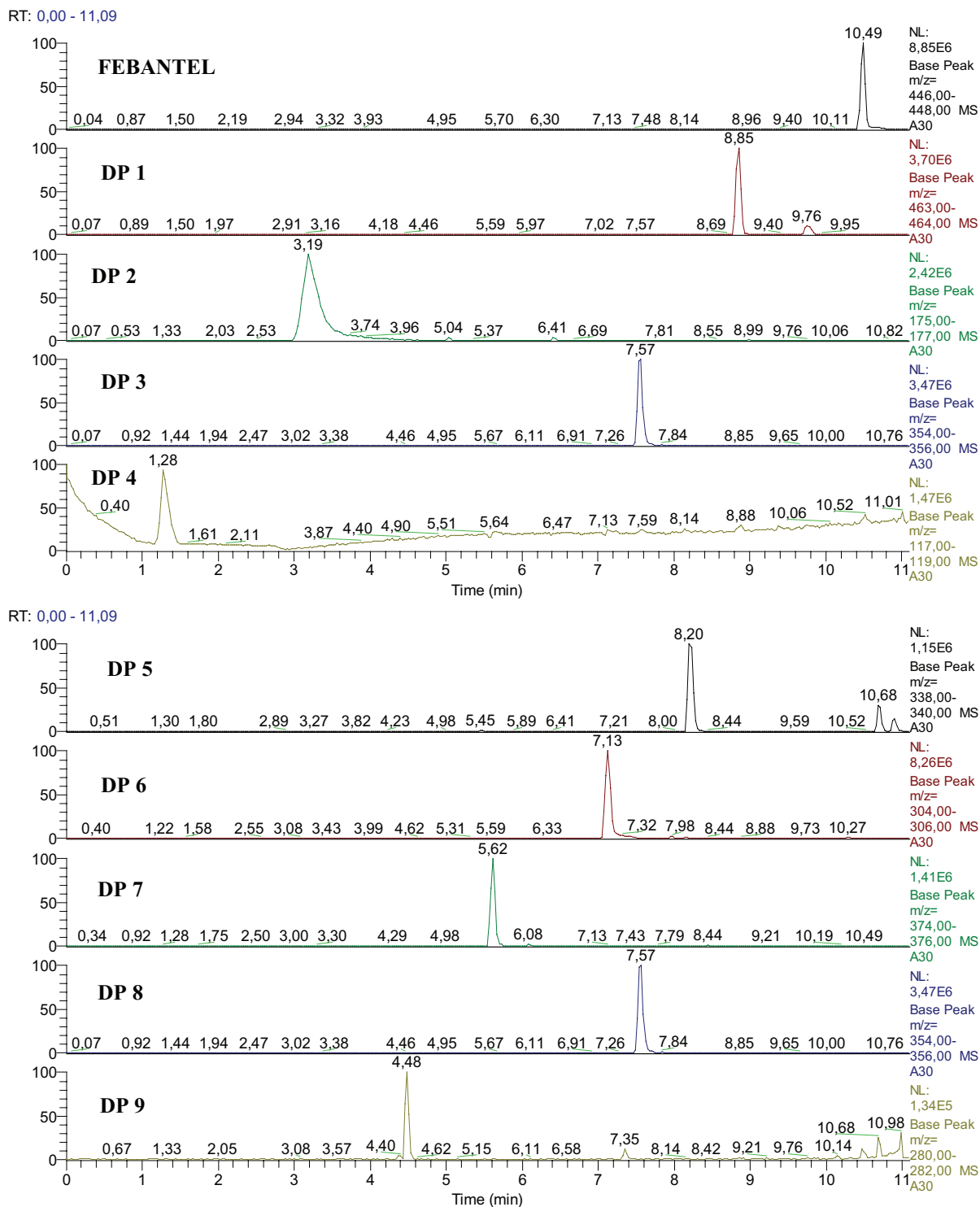


Fig. 2. Chromatogram of sample degraded below 254 nm and with TiO_2 film after 30 min.

m/z 405 for 42 mass units lower in comparison with febantel. The compound DP9 having molecular ion m/z 281 has been obtained as the consequence of the sulfur–carbon bond cleavage inside the diphenylsulfide part of DP8.

The collision induced dissociation of degradation products (DP1–DP9) revealed a facile loss of methanol, thus

confirming the presence of methoxy group in proposed structures. In addition, the cyclization of the primary photodegradation products DP6 and DP7 to stable aromatized systems was observed. Accurate masses of identified febantel degradation products and fragmentation ions are shown in Table 2.

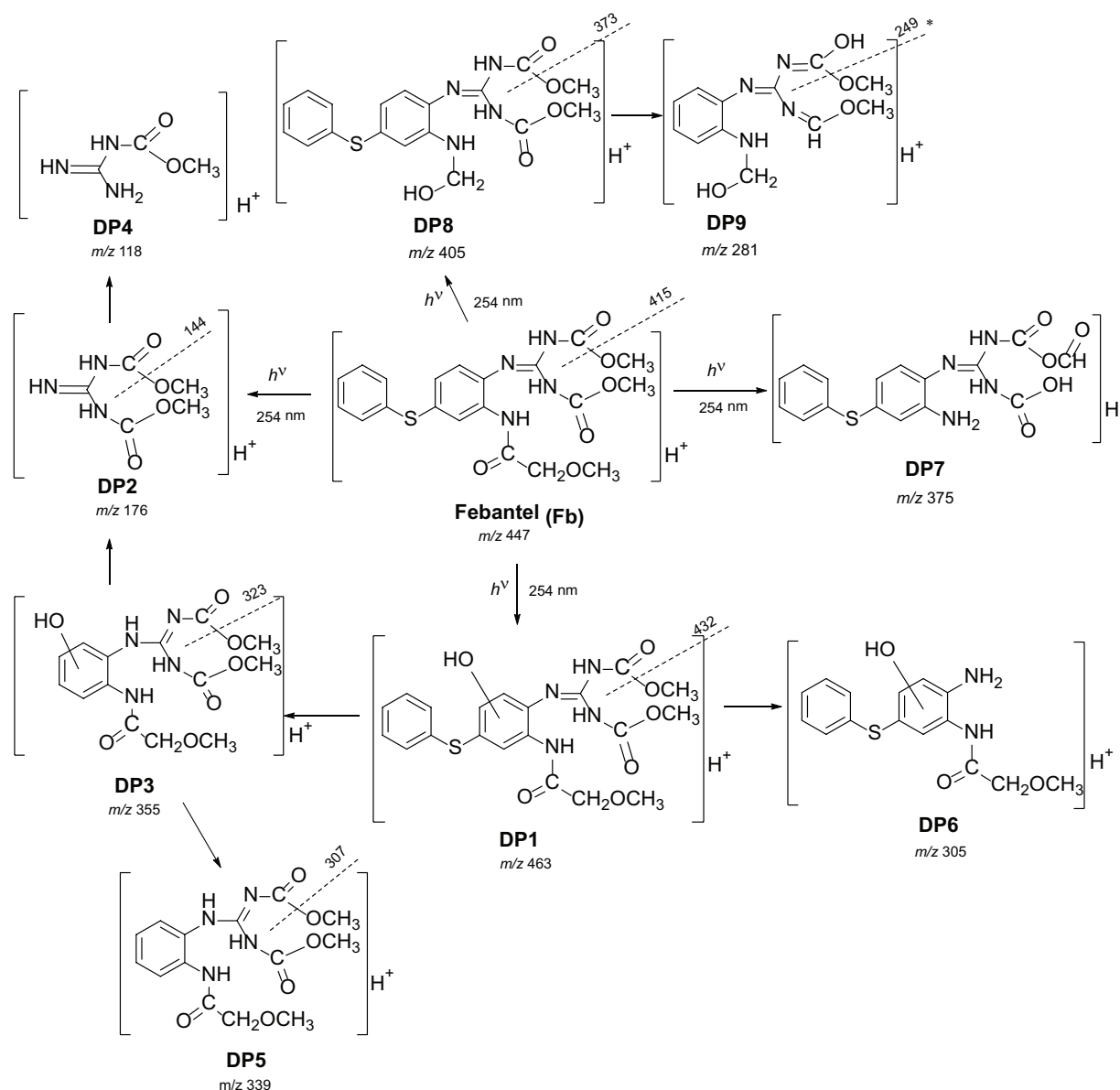


Fig. 3. Tentative molecular structures of febanfel photodegradation products.

Photocatalytic degradation with irradiation of 254 nm proved to be the most efficient for degradation of febanfel and was therefore used to investigate newly formed degradation products. During the first 60 min of the degradation process all the detected degradation products are present (Fig. 4). After 180 min of photocatalytic process all the degradation products are eliminated except for DP4 and DP2, the degradation products with the lowest molecular mass.

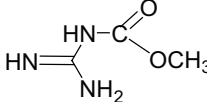
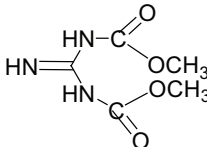
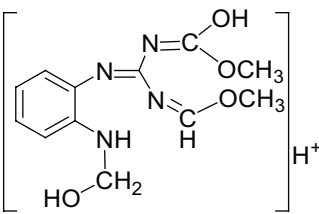
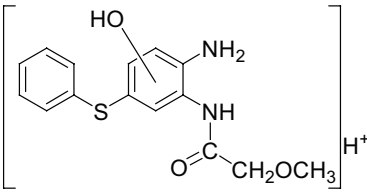
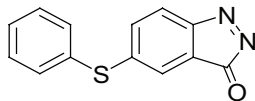
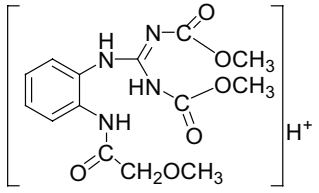
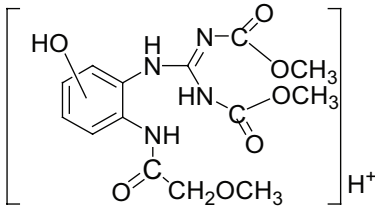
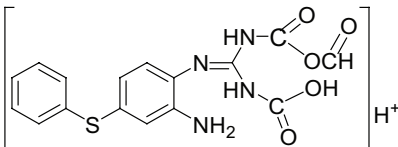
The change of irradiation source to 365 nm yielded different results. During the photocatalysis with 365 nm the same degradation products were formed as with 254 nm except for DP9 which did not appear. DP9 is a result of degradation of DP8 and considering that 365 nm has lower energy it is probable that the degradation efficiency was not enough to degrade DP8 to DP9. Generally, in photocatalysis with irradiation of 365 nm the efficiency of the degradation process was significantly lower since energy from radiation source was

not sufficient to degrade febanfel and degradation products to compounds with smaller molecular mass.

3.3. Toxicity evaluation of samples during the photocatalytic degradation

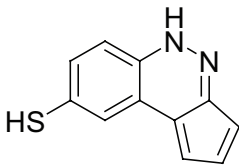
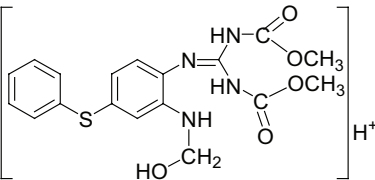
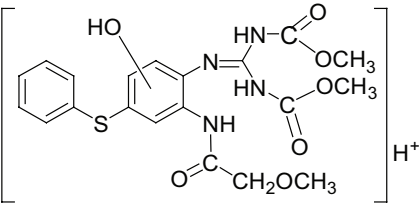
Toxicities of febanfel and the mixtures of its degradation products were evaluated by measuring luminescence inhibition of *Vibrio fischeri* in the samples taken at particular time during photocatalytic process with UV-C radiation. The starting concentration of febanfel in aqueous solution was 10 mg L⁻¹ and samples were taken every 30 min during photocatalytic degradation up to 240 min. Table 3 presents the percentage of luminescence inhibition (*I*, %), 20% and 50% bioluminescence inhibition (EC₂₀ and EC₅₀, mg L⁻¹) values calculated from inhibition curve and the toxicity impact index TII₅₀. Toxicity impact index is defined as (TII = 100(EC₅₀)⁻¹) [28].

Table 2
Accurate masses of febantel degradation products and their fragmentation ions

Name	[M + H] ⁺	Molecular formula	Delta, ppm	RDB ^a	Molecular structure
DP4	118.06113	C ₃ H ₈ O ₂ N ₃	0.228	1.5	
DP2	176.06645	C ₅ H ₁₀ O ₄ N ₃	-0.751	2.5	
DP9	144.03290	C ₄ H ₆ O ₃ N ₃	-7.468	3.5	
DP9	281.12463	C ₁₂ H ₁₇ O ₄ N ₄	0.706	6.5	
DP6	249.09880	C ₁₁ H ₁₃ O ₃ N ₄	0.583	7.5	
DP6	305.09531	C ₁₅ H ₁₇ O ₃ N ₂ S	-0.425	8.5	
	240.03618	C ₁₃ H ₈ ON ₂ S	0.99	11.0	
DP5	339.12979	C ₁₄ H ₁₉ O ₆ N ₄	-0.356	7.5	
	307.10428	C ₁₃ H ₁₅ O ₅ N ₄	0.584	8.5	
DP3	355.12476	C ₁₄ H ₁₉ O ₇ N ₄	-0.184	7.5	
	323.09942	C ₁₃ H ₁₅ O ₆ N ₄	0.809	8.5	
DP7	375.07614	C ₁₆ H ₁₅ O ₅ N ₄ S	0.995	11.5	

(Continued)

Table 2 (Continued)

Name	[M + H] ⁺	Molecular formula	Delta, ppm	RDB ^a	Molecular structure
	199.03257	C ₁₁ H ₇ N ₂ S	0.12	9.5	
DP8	405.12286	C ₁₈ H ₂₁ O ₅ N ₄ S	0.353	10.5	
DP1	373.09714	C ₁₇ H ₁₇ O ₄ N ₄ S	0.638	11.5	
	463.12802	C ₂₀ H ₂₃ O ₇ N ₄ S	-0.380	11.5	
	432.10617	C ₁₉ H ₂₀ O ₆ N ₄ S	-3.636	12.0	

Note: Bold values indicate that the ions are easily distinguished from fragments.

^aRDB, ring and double-bond equivalents.

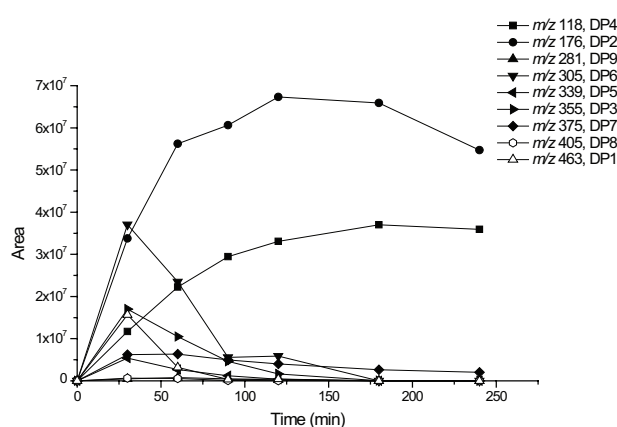


Fig. 4. Degradation profiles of identified degradation products during UV-A + TiO₂ experiment.

Table 3

Toxicity parameters obtained using *Vibrio fischeri* (UV-C photocatalytic degradation, initial concentration of febantel 10 mg L⁻¹)

<i>t</i> , min	<i>I</i> , %	EC _{20'} , mg L ⁻¹	EC _{50'} , mg L ⁻¹	TII ₅₀
0	0	–	–	–
30	11.50	–	–	–
60	85.87	1.99	2.5	40.0
90	93.50	1.50	1.89	52.9
120	94.56	1.30	1.60	62.5
180	98.43	0.50	0.65	153.9
240	98.28	0.60	1.50	66.7

From the results in Table 3, it can be seen that 10 mg L⁻¹ solution of febantel prior to the photocatalysis is not toxic. The first solution, which indicates luminescence inhibition of *Vibrio fischeri* was solution sampled after 30 min (*I* = 11.5%), and for that the sample was not possible to determine the EC₂₀ and EC₅₀ values from inhibition curve. However, the sample sampled at 60th minute showed very high luminescence inhibition (85.9%), whereby luminescence inhibition grows to 98.3% for sample sampled at 240th minute. Results for toxicity evaluation may be correlated with the degradation products profiles shown in Fig. 4. Hence, it can be concluded that luminescence inhibition increases with the concentration of degradation products *m/z* 118 and 176, while the concentration of other degradation products decreases to minimum. The highest value of toxicity impact index (TII₅₀ = 153.9) is for sample sampled at 180th minute where degradation products *m/z* 118 and 176 are at their maximum. After 180 min toxicity impact index shows a decrease.

4. Conclusions

This study investigates degradation kinetics of febantel during photolysis (UV-A or UV-C radiation) and photocatalysis (UV-A radiation + TiO₂ or UV-C radiation + TiO₂). Degradation of febantel occurred in all experiments except during the photolysis by UV-A radiation. Kinetic study showed that for all experiments degradation followed pseudo-first-order reaction kinetics. The most efficient degradation process proved to be photocatalysis with predominant light of 254 nm with TiO₂ in a form of a sol-gel thin film during which febantel was degraded in less than 20 min.

High resolution mass spectrometry was used to detect and identify degradation products. During the photocatalytic

degradation nine degradation products were identified in total, during 254 nm + TiO₂ process. All detected degradation products were degraded during the period of 180 min except DP2 and DP4 most likely because more efficient degradation is necessary to degrade smaller molecules. After 90 min of photocatalytic degradation with 365 nm the same degradation products were formed except DP9. Also, predominant degradation products were those with higher molecular mass.

Degradation pathways and tentative structural formulae of degradation products were proposed based on mass spectral data and the principle of photocatalysis. The main processes of degradation are the hydroxylation of the phenyl ring of febantel besides methoxyacetamide substituent reduction in febantel. The degradation paths include the cleavage of carbon–sulfur bond in the diphenylsulfide part of the structure, than consequent disappearance of the carbamate side chain and the final reduction step. The obtained results revealed that investigated febantel underwent rapid photodegradation to the related phenol, carboxy, hydroxy and carbamate derivatives.

Toxicity test with *Vibrio fischeri* has shown that samples after 60 and 240 min of degradation process indicated a higher toxicity primarily due to degradation products DP4 (molecular mass of 118.06113) and DP2 (molecular mass of 176.06645). Also, after 180 min TII₅₀ indicates that the toxicity reduces as degradation products are being degraded.

Acknowledgment

This study has been supported by the Croatian Science Foundation under the project Fate of pharmaceuticals in the environment and during advanced wastewater treatment (*PharmaFate*) (IP-09-2014-2353).

References

- [1] B. Halling-Sørensen, S.N. Nielsen, P.F. Lanzky, F. Ingerslev, H.C.H. Lützhøft, S.E. Jørgensen, Occurrence, fate and effects of pharmaceutical substances in the environment – a review, *Chemosphere*, 36 (1998) 357–393.
- [2] K. Kümmeler, *Pharmaceuticals in the Environment*, Springer Verlag, Berlin, 2008.
- [3] W.C. Li, Occurrence, sources, and fate of pharmaceuticals in aquatic environment and soil. *Environ. Pollut.*, 187 (2014) 193–201.
- [4] P. Bottoni, S. Caroli, A.B. Caracciolo, Pharmaceuticals as priority water contaminants, *Toxicol. Environ. Chem.*, 92 (2010) 549–565.
- [5] C.G. Daughton, T. Ternes, Pharmaceuticals and personal care products in the environment: agents of subtle change? *Environ. Health Perspect.*, 107 (1999) 907–938.
- [6] A.K. Sarmah, M.T. Meyer, A.B.A. Boxall, A global perspective on the use, sales, exposure pathways, occurrence, fate and effects of veterinary antibiotics (VAs) in the environment, *Chemosphere*, 65 (2006) 725–759.
- [7] J.W. Tracy, L.T. Webster, Jr., *Drugs Used in the Chemotherapy of Helminthiasis*, J.G. Hardman, L.E. Limbird, Eds., Goodman and Gilman's The Pharmacological Basis of Therapeutics, McGraw-Hill, New York, 2001.
- [8] R. Kreuzig, S. Höltge, J. Brunotte, N. Berenzen, J. Wogram, R. Schulz, Test plat studies on runoff of sulfonamides from manured soil after sprinkler irrigation, *Environ. Toxicol. Chem.*, 24 (2005) 777–781.
- [9] Q.A. Mckellar, F. Jackson, Veterinary anthelmintics: old and new, *Trends Parasitol.*, 20 (2004) 456–461.
- [10] W. Sim, H. Kim, S. Choi, J. Kwon, J. Oh, Evaluation of pharmaceuticals and personal care products with emphasis on anthelmintics in human sanitary waste, sewage, hospital wastewater, livestock wastewater and receiving water, *J. Hazard. Mater.*, 248–249 (2013) 219–227.
- [11] A.J.M. Horvat, S. Babić, D.M. Pavlović, D. Ašperger, S. Pelko, M. Kaštelan-Macan, M. Petrović, A.D. Mance, Analysis, occurrence and fate of anthelmintics and their transformation products in the environment, *TrAC, Trends Anal. Chem.*, 31 (2012) 61–84.
- [12] K. Weiss, W. Schüssler, M. Porzelt, Sulfamethazine and flubendazole in seepage water after the sprinkling of manured areas, *Chemosphere*, 72 (2008) 1292–1297.
- [13] K.A. Krogh, E. Björklund, D. Löffler, G. Fink, B. Halling-Sørensen, T.A. Ternes, Development of an analytical method to determine avermectins in water, sediments and soils using liquid chromatography–tandem mass spectrometry, *J. Chromatogr., A*, 1211 (2008) 60–69.
- [14] D.A. Alvarez, P.E. Stackelberg, J.D. Petty, J.N. Huckins, E.T. Furlong, S.D. Zaugg, M.T. Meyer, Comparison of a novel passive sampler to standard water-column sampling for organic contaminants associated with wastewater effluents entering a New Jersey stream, *Chemosphere*, 61 (2005) 610–622.
- [15] J.C. Van da Steene, W.E. Lambert, Validation of a solid-phase extraction and liquid chromatography–electrospray tandem mass spectrometric method for the determination of nine basic pharmaceuticals in wastewater and surface water samples, *J. Chromatogr., A*, 1182 (2008) 153–160.
- [16] M. Zrnčić, M. Gros, S. Babić, M. Kaštelan-Macan, D. Barcelo, M. Petrović, Analysis of anthelmintics in surface water by ultra high performance liquid chromatography coupled to quadrupole linear ion trap tandem mass spectrometry, *Chemosphere*, 99 (2014) 224–232.
- [17] R.R. Giri, H. Ozaki, S. Ota, R. Takanami, S. Taniguchi, Degradation of common pharmaceuticals and personal care products in mixed solutions by advanced oxidation techniques, *Int. J. Environ. Sci. Technol.*, 7 (2010) 251–260.
- [18] M. Chaudhuri, E.S. Elmolla, Photocatalytic degradation of amoxicillin, ampicillin and cloxacillin antibiotics in aqueous solution using UV/TiO₂ and UV/H₂O₂/TiO₂ photocatalysis, *Desalination*, 252 (2010) 46–52.
- [19] L. Curković, D. Ljubas, S. Šegota, I. Bačić, Photocatalytic degradation of Lissamine Green B dye by using nanostructured sol-gel TiO₂ films, *J. Alloys Compd.*, 604 (2014) 309–316.
- [20] S. Šegota, L. Curković, D. Ljubas, V. Svetličić, I.F. Houra, N. Tomašić, Synthesis, characterization and photocatalytic properties of sol-gel TiO₂ films, *Ceram. Int.*, 37 (2011) 1153–1160.
- [21] H.J. Kuhn, S.E. Braslavsky, R. Schmidt, *Chemical Actinometry* (IUPAC Technical Report), *Pure Appl. Chem.*, 76 (2004) 2105–2146.
- [22] M. Katajamaa, J. Miettinen, M. Orešič, MZmine: Toolbox for processing and visualization of mass spectrometry based molecular profile data, *Bioinformatics*, 22 (2006) 634–636.
- [23] M. Rožman, M. Petrović, Bquant – novel script for batch quantification of LCMS data, *MethodsX*, 3 (2016) 520–524.
- [24] M.R. Hoffmann, S.T. Martin, W. Choi, D.W. Bahnemann, Environmental applications of semiconductor photocatalysis, *Chem. Rev.*, 95 (1995) 69–96.
- [25] O. Legrini, E. Oliveros, A.M. Braun, Photochemical processes for water treatment, *Chem. Rev.*, 1993 (1993) 671–698.
- [26] C.S. Truchi, D.F. Ollis, Degradation of organic water contaminants: mechanisms involving hydroxyl radical attack, *J. Catal.*, 122 (1990) 178–192.
- [27] T. Oppenländer, *Photochemical Purification of Water and Air – Advanced Oxidation Processes (AOPs): Principles, Reaction Mechanisms, Reactor Concepts*, Wiley-VCH, Weinheim, 2003.
- [28] M. Farre, D. Ašperger, L. Kantiani, S. Gomez, M. Petrović, D. Barcelo, Assessment of the acute toxicity of triclosan and methyl triclosan in wastewater based on bioluminescence inhibition of *Vibrio fischeri*, *Anal. Bioanal. Chem.*, 390 (2008) 1999–2007.

Supplementary material

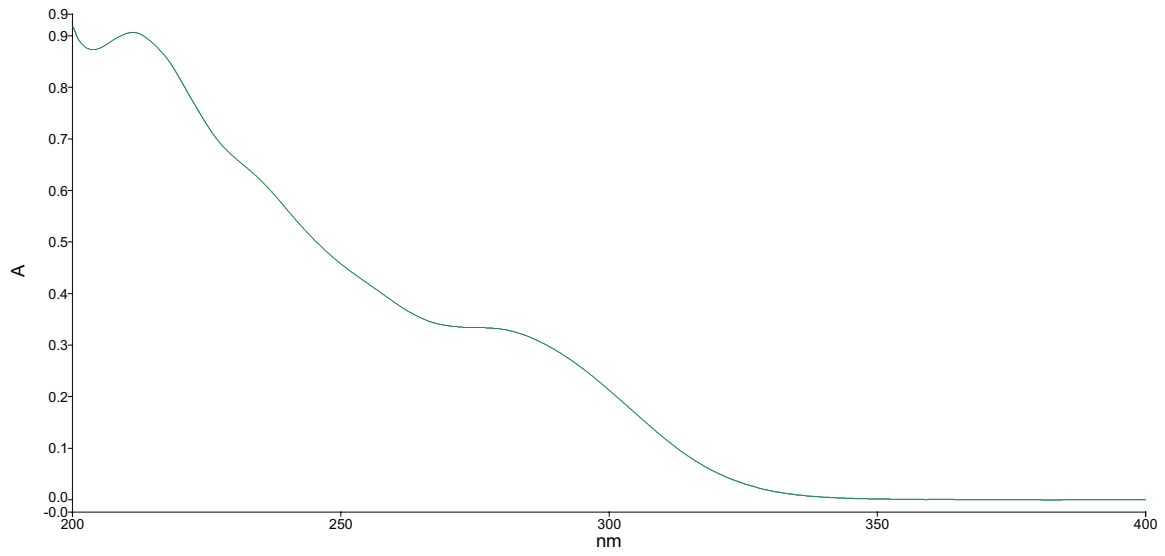


Fig. S1. Absorption spectra of febantel.